Frequency Estimation for Sychrophasor Measurement Units in Power System

Luoyang Fang and Liuqing Yang
Department of Electrical and Computer Engineering
Colorado State University

Abstract

Frequency estimation is a crucial signal processing technique in Phasor Measurement Units (PMU). In this report, we propose a new algorithm for frequency estimation by interpolation of zero-padded discrete Fourier transform (DFT) samples. The bias performance of the proposed estimator is analyzed and an iterative algorithm is further proposed to reduce the bias to an arbitrarily small level. Simulations show that our proposed algorithm have the best performance among existing ones in the literature. In addition, the performance of our algorithm can satisfy the requirements of standard C37.118.1, with short observation windows.

I. Introduction

Frequency is very important parameter for monitoring the status of the power system. A deviation of frequency from the system nominal frequency demonstrates an unbalance between the generated power and the power consumption of the load [1]. Modern power systems maintain the power balance by monitoring the system frequency. In next generation smart power grid, wide area measurement system with many more advanced measurement devices will be developed to estimate the system state, monitor and protect the power system. This requires accurate parameter measurements, such as amplitude, phase, and frequency. In fact, a lot of algorithms for phasor (amplitude and phase) measurement are based on the prior knowledge of the true frequency. Therefore, the accuracy of frequency estimation will further influence the accuracy of the phasor measurement.

In 2005, IEEE power engineering society presented standard C37.118 [2] to define phasor measurement, and to provide a method of quantifying the measurements and quality test specifications. Two new standards C37.118.1 [3] and C37.118.2 [4], which were modified version of C37.118 [2], were published in 2011. In [3], synchronized phasor and frequency measurements at substations along with methods and requirements for measurement verification are defined. Communication and recording of phasor measurements are covered in [4]. In the new standard [3], frequency estimation requirements were first introduced.

Sampling and windowing can not be avoided, and windowing in the time domain will definitely lead to spectrum leakage, which then result in inaccuracies in the estimation. After taking discrete Fourier transform (DFT), spectrum leakage will also affect the accuracy of phasor measurement. There are several factors which influence the performance of frequency estimation, such as window length, zero padding, and so on. Analysis of these parameters will give insight to the design of estimation algorithms. This report will focuses on frequency estimation for PMU. In addition, the effect of the stated parameters will be investigated and an algorithm for frequency estimation will be proposed. Finally, simulations are performed to test its performance in accordance with the standard.

II. SIGNAL MODEL

Defined in standard [3], power signals are modeled as real sinusoidal signal as follows:

$$\begin{aligned} x(t) &= A\cos(2\pi ft+\phi) \\ &= A\cdot \mathrm{Re}\left\{\mathrm{e}^{j(2\pi ft+\phi)}\right\} \end{aligned}$$

where f is the signal frequency to be estimated, A and ϕ are the unknown magnitude and initial phase respectively. Also, $\mathrm{Re}\{\cdot\}$ means the real part operation. In a balanced three-phase power system, it can be proved that the positive sequence of the system is the complex sinusoidal signal. Hence, the real sinusoidal signal model can be simplified to the complex sinusoidal one as follows:

$$x(t) = A\mathrm{e}^{j(2\pi ft+\phi)} + w(t) \tag{1}$$

Where $w(t)$ is the additive complex white Gaussian noise. In real applications, the measurement device will only obtain a discretely-sampled and finite-windowed version of the original signal. In this report, the simplest rectangular window is adopted. Denote the sampling frequency as f_s and window length N. Then the signal observed will be represented as follows:

$$\begin{aligned} \text{After Sampling: } x(nT_s) &= A\mathrm{e}^{j(2\pi fnT_s+\phi)} + w(nT_s) \\ \text{After Discretization: } x[n] &= A\mathrm{e}^{j(2\pi \frac{f}{f_s}n+\phi)} + w[n] \end{aligned} \tag{2}$$

where $T_s = \frac{1}{f_s}$.

After an M-point DFT, the representation of the signal in the frequency domain is :

$$\begin{aligned} X[k] &= \sum_{n=0}^{N-1} A\mathrm{e}^{j\phi}\mathrm{e}^{j2\pi\frac{f}{f_s}n}\mathrm{e}^{-j\frac{2\pi}{M}nk} + W[k] \\ &= A\mathrm{e}^{j\phi}\mathrm{e}^{j\pi(N-1)(\frac{f}{f_s}-\frac{k}{M})}\frac{\sin\left(\pi N(\frac{f}{f_s}-\frac{k}{M})\right)}{\sin\left(\pi(\frac{f}{f_s}-\frac{k}{M})\right)} + W[k] \end{aligned} \tag{3}$$

where M is the number of samples in the frequency domain with $M \geq N$. If $M > N$, $(M-N)$ zeros need to be padded to the original observations before DFT. $W[k]$ is the representation of the noise in the frequency domain, which will be white if $M = N$ and colored if $M > N$. Notice that the DFT samples, $X[k]$, are a sampled version of the discrete-time Fourier transform (DTFT) of the original signal and the relationship between the index k and the frequency in DTFT is $f_{\mathrm{DTFT}} = k\frac{f_s}{M} = k\Delta f$, where Δf is the DFT resolution. Generally, no DFT samples will correspond to the true frequency of the system. In other words, there is usually a gap δ between the original frequency and the location of the maximum DFT sample.

$$f = (k_m+\delta)\Delta f \tag{4}$$

where k_m is the index of the maximum DFT point. Substituting Eq. (4) into Eq. (3), we obtain:

$$X[k_m+i] = A\mathrm{e}^{j\phi}\mathrm{e}^{j\pi\frac{N-1}{M}(\delta-i)}\frac{\sin\left(\frac{\pi N}{M}(\delta-i)\right)}{\sin\left(\frac{\pi}{M}(\delta-i)\right)} + W[i]\ , \tag{5}$$

where i denotes the distance of index from the maximum. An illustration of the signal model can be also found in Fig. 1.

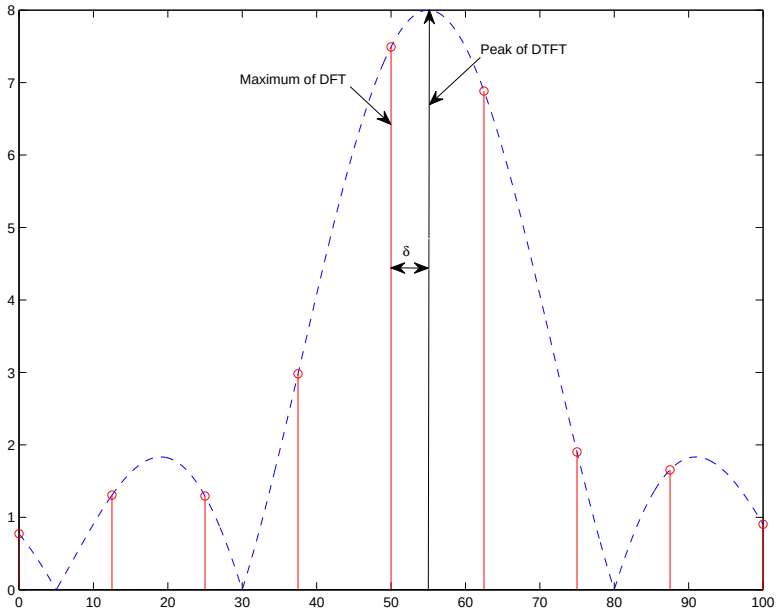

Fig. 1. Ideal spectrum (impulse), DTFT (dashed line) and DFT samples of $x(t) = e^{j(2\pi \times 55t)}$ with sampling frequency $f_s = 50$ Hz, observation window size $N = 8$ and DFT size $M = 16$ (only 9 points are shown).

III. Analysis

A. Fisher Information Matrix and Cramer-Rao Lower Bound

In parameter estimation, a criteria is vital to determine which is the best estimator based on the available data. Generally, root mean square error (RMSE) is a good metric to compare methods of estimation and to determine the best one. In addition, Cramer-Rao (CR) lower bound defines the theoretically best mean square error (MSE) of an estimation for a given Signal-to-noise ratio (SNR) and available data. For the case of frequency estimation of a signal-tone complex sinusoidal signal, the CR lower bound was first introduced in 1974 [5]. As stated in [5], the unbiased CR bounds are the diagonal elements of the inverse of the Fisher information Matrix $\mathbf{J}$ whose elements are given by

$$\mathbf{J}_{ij} = \mathbf{E}\{H_{\alpha_i} H_{\alpha_j}\} = -\mathbf{E}\{H_{\alpha_i} H_{\alpha_j}\} \tag{6}$$

where

$$H_{\alpha_i} = \frac{\partial}{\partial \alpha_i} \log p(Z; \alpha) \tag{7}$$

Here α is the parameters to be estimated and Z is the observations and $p(Z; \alpha)$ is probability distribution function of Z assuming that α is given. In our frequency estimation case, $\alpha = [\omega, A, \phi]$, if the magnitude and angle are unknown. Bounds are given below:

$$\text{var}\{\hat{\alpha_i}\} \quad \geq \quad [\mathbf{J}^{-1}]_{ii} \tag{8}$$

Where $\mathbf{J}^{-1}$ is the inverse of the Fisher Information matrix $\mathbf{J}$. For the case where only the frequency is unknown, the CR bound for frequency estimation is shown to be

$$\begin{aligned} \mathrm{var}\{\hat{\omega}\} &\geq \frac{6f_s^2\sigma^2}{A^2N(N^2-1)} \\ \mathrm{var}\{\hat{f}\} &\geq \frac{6f_s^2}{4\pi^2\gamma N(N^2-1)} \end{aligned} \tag{9}$$

where N is the number of samples and $\gamma = \frac{A^2}{\sigma^2}$ is the Signal-to-noise ratio. This result was proposed in [6]. As Eq. (9) shows, increasing the observation window length will reduce the lower bound, which means longer observation window would helps improve the performance of the estimator. Moreover, SNR is another important parameter affecting performance of the estimator, as showed in Eq. (9).

B. Effect of Zero-padding on Imposed Noise

The spectrum of sinusoidal depends on observation windows length. However, the number of samples in the frequency spectrum not only relies on the number of samples in the time domain, but is also on number of padding zeros. Therefore, zero-padding is one technique to increase frequency resolution without enlarging the observation window. Here is mathematical expression for the zero-padding:

$$x_M[n] = \begin{cases} x[n] & \text{if } 0 \leq n < N \\ 0 & \text{if } N \leq n < M-1 \end{cases}$$

The higher frequency resolution means that $\Delta f = \frac{f_s}{M}$ is smaller. As Fig. 1 shows, the maximum sample on the frequency domain will be close to the peak value. As showed in equation (2), the noise part is the white gaussian with zero mean and σ^2 variance. After the DFT, the noise would be as follows without zero-padding

$$W[k] = \sum_{n=0}^{N-1} \mathrm{e}^{j\frac{2\pi}{N}kn} w[n] \tag{10}$$

where $W[k]$ is the k-th noise imposed on the k-th sample of the signal in the frequency domain, and its mean and variance are

$$\mathrm{Mean}\{W[k]\} = \mathbf{E}\{W[k]\} = \mathbf{E}\left\{\sum_{n=0}^{N-1} \mathrm{e}^{-j\frac{2\pi}{N}kn} w[n]\right\} = \sum_{n=0}^{N-1} \mathrm{e}^{-j\frac{2\pi}{N}kn}\mathbf{E}\{w[n]\} = 0 \tag{11}$$

$$\mathrm{Var}\{W[k]\} = \mathbf{E}\{W[k]W^*[k]\} = \sum_{n=0}^{N-1} \mathrm{e}^{-j\frac{2\pi}{N}kn}\mathrm{e}^{j\frac{2\pi}{N}kn}\mathbf{E}\{w^2[n]\} = N * \mathbf{E}\{w^2[n]\} = N\sigma^2 \tag{12}$$

where $\{\cdot\}^*$ denotes the comlex conjugate of $\{\cdot\}$. Also, in the frequency domain, the noises experienced by samples is independent when non-zero-padding is used. The covariance of $W[k]$ is

$$\mathbf{E}\{W[k]W^*[k+l]\} = \sum_{n=0}^{N-1}\{\mathrm{e}^{-j\frac{2\pi}{N}kn}\mathrm{e}^{j\frac{2\pi}{N}(k+l)n}\}\mathbf{E}\{w^2[n]\} = \frac{1-\mathrm{e}^{j2\pi l}}{1-\mathrm{e}^{j\frac{2\pi}{N}l}} * \sigma^2 \tag{13}$$

From Eq. (13), when $l = 0$, the covariance becomes the variance of $W[k]$, $\mathbf{E}\{W[k]W^*[k]\} = N\sigma^2$. When $l \neq 0$, the numerator of Eq. (13) is 0, but the denominator is not zero. Hence, $\mathbf{E}\{W[k]W^*[k+l]\} = 0$. However,when zero-padding is used, the noise in the frequency domain is correlated, which means the noise is no longer white. In this case, the covariance $W[k]$ is given by:

$$\mathbf{E}\{W[k]W^*[k+l]\} = \sum_{n=0}^{N-1}\{\mathrm{e}^{-j\frac{2\pi}{M}kn}\mathrm{e}^{j\frac{2\pi}{M}(k+l)n}\}\mathbf{E}\{w^2[n]\} = \frac{1-\mathrm{e}^{j\frac{2\pi N}{M}l}}{1-\mathrm{e}^{j\frac{2\pi}{M}l}} * \sigma^2 \tag{14}$$

where M can be $2N, 3N$ or $4N$. Note, $\mathbf{E}\{W[k]W^*[k+l]\}$ is not always equal to zero, when $l \neq 0$. For example, let $M = 2N$, we can get the covariance of two noises in the frequency domain:

$$\mathbf{E}\{W[k]W^*[k+l]\} = \begin{cases} N\sigma^2 & \text{if } l = 0 \\ \frac{2}{1-\mathrm{e}^{\pm j\frac{2\pi}{M}}} & \text{if } l = \pm 1 \\ 0 & \text{if } l \neq 0 \text{ and } l \neq \pm 1 \end{cases}$$

In summary, zero padding will help increase frequency resolution,which will reduce the bias of the estimator in some algorithms, but it leads to colored noise in the frequency domain.

IV. Proposed Algorithm of Frequency Estimation

A. proposed algorithm

From Fig. 1, the relationship between the location of the maximum of DFT and peak of DFTF was clearly demonstrated. Therefore, frequency estimation of single-tone complex sinusoidal signal can be summarized as two stage. The first stage is to locate maximum samples on frequency domain after DFT. And then, a fine search is performed to estimate the frequency gap δ between the true frequency and the maximum of DFT in second stage. Our proposed method contributes to the second stage. For simplicity, the algorithm development will be stated starting from the noiseless case.

By taking the magnitude of the DFT samples , we are able to remove the unknown phase parameter ϕ. From Eq. (5), let $M = 2N$ and $i = \pm 1$, the magnitudes of the two neighbors of the maximum are:

$$|X[k_m + 1]| = A\frac{\sin(\frac{\pi}{2}(1-\delta))}{\sin(\frac{\pi}{M}(1-\delta))} = A\frac{\cos(\frac{\pi}{2}\delta)}{\sin(\frac{\pi}{M}(1-\delta))} \tag{15}$$

$$|X[k_m - 1]| = A\frac{\sin(\frac{\pi}{2}(1+\delta))}{\sin(\frac{\pi}{M}(1+\delta))} = A\frac{\cos(\frac{\pi}{2}\delta)}{\sin(\frac{\pi}{M}(1+\delta))} \tag{16}$$

By our definitions, for any signal, the frequency gap is $-0.5 \leq \delta \leq 0.5$. Moreover, in real applications, generally we have $M \geq 4$. As a result, $0 < \frac{\pi}{M}(1 \pm \delta) < \frac{\pi}{2}$

When the same number of zeros as the observation window size is appended, the width of the main lobe of the DTFT spectrum is $\frac{2}{N} \times f_s$ and the frequency resolution is $\Delta f = \frac{f_s}{M} = \frac{1}{2N} \times f_s$. Therefore, the number of samples in the main lobe is $\frac{\frac{2}{N}\times f_s}{\frac{1}{2N}\times f_s} = 4$ as shown in Fig. 1. As a result, in the noiseless case, $|X[k_m \pm 1]|$ will never be zero-valued. By taking the ratio of the magnitude of the two neighboring DFT samples of the maximum, we can further remove the unknown magnitude parameter, A, from the frequency estimation process. Accordingly, by Eq. (15) and (16),

$$\alpha = \left|\frac{X[k_m + 1]}{X[k_m - 1]}\right| = \frac{\sin(\frac{\pi}{M}(1+\delta))}{\sin(\frac{\pi}{M}(1-\delta))} \tag{17}$$

As shown above, α only contains the information of δ which indicates the true frequency location. Using a trigonometric identity, Eq. (17) can be further expanded as follows:

$$\begin{aligned} \alpha &= \frac{\sin\frac{\pi}{M}\cos\frac{\pi}{M}\delta + \cos\frac{\pi}{M}\sin\frac{\pi}{M}\delta}{\sin\frac{\pi}{M}\cos\frac{\pi}{M}\delta - \cos\frac{\pi}{M}\sin\frac{\pi}{M}\delta} \\ &= \frac{\tan\frac{\pi}{M} + \tan\frac{\pi}{M}\delta}{\tan\frac{\pi}{M} - \tan\frac{\pi}{M}\delta} \end{aligned} \tag{18}$$

Since $0 \leq \frac{\pi}{M}\delta < \frac{\pi}{2}$, we have $\cos\left(\frac{\pi}{M}\delta\right) \neq 0$, and since $0 < \frac{\pi}{M} < \frac{\pi}{2}$, we also have $\cos\left(\frac{\pi}{M}\right) \neq 0$. Therefore, $\tan\left(\frac{\pi}{M}\delta\right)$ can be obtained by Eq. (18) as follows:

$$\tan\left(\frac{\pi}{M}\delta\right) = \tan\left(\frac{\pi}{M}\right) \cdot \frac{\alpha - 1}{\alpha + 1} \tag{19}$$

Since $\frac{\pi}{M}\delta$ is very small, the approximation $\tan\left(\frac{\pi}{M}\delta\right) = \frac{\pi}{M}\delta$ can be applied to obtain an estimate of δ in closed-form expression as follows:

$$\hat{\delta} = \frac{\tan(\pi/M)}{\pi/M} \cdot \frac{\alpha - 1}{\alpha + 1} = \frac{\tan(\pi/M)}{\pi/M} \frac{|X[k_m + 1]| - |X[k_m - 1]|}{|X[k_m + 1]| + |X[k_m - 1]|} \tag{20}$$

Accordingly, by Eq. (4), the frequency estimator is

$$\hat{f} = (k_m + \hat{\delta})\frac{f_s}{M} \, . \tag{21}$$

B. Bias Analysis and Proposed Bias-compensated Algorithm

As there is an approximation in the development of the proposed algorithm, the estimator will be biased. The Taylor expansion of $\tan\left(\frac{\pi}{M}\delta\right)$ from Eq. (19) is as follows:

$$\tan\left(\frac{\pi}{M}\delta\right) = \frac{\pi}{M}\delta + \frac{1}{3}\left(\frac{\pi}{M}\right)^3\delta^3 + \frac{2}{15}\left(\frac{\pi}{M}\right)^5\delta^5 + \text{h. o. t.}$$

where h.o.t. stands for higher order terms. Therefore, in the noise-free situation,

$$b_\delta = \hat{\delta} - \delta = \frac{1}{3}\left(\frac{\pi}{M}\right)^2\delta^3 + \frac{2}{15}\left(\frac{\pi}{M}\right)^4\delta^5 + \text{h. o. t.} \approx \frac{1}{3}\left(\frac{\pi}{M}\right)^2\delta^3 \tag{22}$$

The explicit closed-form expression of the true value of δ can be obtained from our proposed algorithm as:

$$\begin{aligned} \delta &= \frac{1}{\pi/M}\arctan\left(\tan(\pi/M)\frac{\alpha - 1}{\alpha + 1}\right) \\ &= \frac{1}{\pi/M}\arctan\left(\tan(\pi/M)\frac{|X[k_m + 1]| - |X[k_m - 1]|}{|X[k_m + 1]| + |X[k_m - 1]|}\right) \end{aligned} \tag{23}$$

Denote $\theta = \tan(\pi/M)\frac{|X[k_m+1]|-|X[k_m-1]|}{|X[k_m+1]|+|X[k_m-1]|}$, and the Taylor expansion of $\arctan$ at zero is:

$$\arctan(\theta) = \theta - \frac{1}{3}\theta^3 + \frac{1}{5}\theta^5 - \frac{1}{7}\theta^7 + \cdots + (-1)^{(n-1)/2}\frac{1}{n}\theta^n + \cdots \tag{24}$$

where $n \in \{1, 3, 5, 7, \dots\}$.Hence, the estimator of the bias-compensated algorithm can be written from Eq. (24) as:

$$\hat{\delta}_i = \frac{M}{\pi}\theta - \frac{1}{3}\frac{M}{\pi}\theta^3 + \frac{1}{5}\frac{M}{\pi}\theta^5 - \frac{1}{7}\frac{M}{\pi}\theta^7 + \cdots + (-1)^{(n-1)/2}\frac{1}{n}\frac{M}{\pi}\theta^n \tag{25}$$

where $n = 2i - 1$. Substituting the original estimator, $\theta = \frac{\pi}{M}\hat{\delta}$, into Eq. (25), the iterative algorithm can be obtained as:

$$\hat{\delta}_i = \hat{\delta} - \frac{1}{3}(\frac{\pi}{M})^2\hat{\delta}^3 + \frac{1}{5}(\frac{\pi}{M})^4\hat{\delta}^5 + \cdots + (-1)^{(n-1)/2}\frac{1}{n}(\frac{\pi}{M})^{(n-1)}\hat{\delta}^n + \cdots \tag{26}$$

The iterative bias-compensated estimator is as follows:

$$\hat{f}_i = (k_m + \hat{\delta}_i)\frac{f_s}{M}. \tag{27}$$

Finally, the procedure of our proposed algorithm is summarized in Fig. 2.

V. Simulation

In this section, the general performance of our proposed algorithm is investigated and the parameter setting are given, according to standard [3].

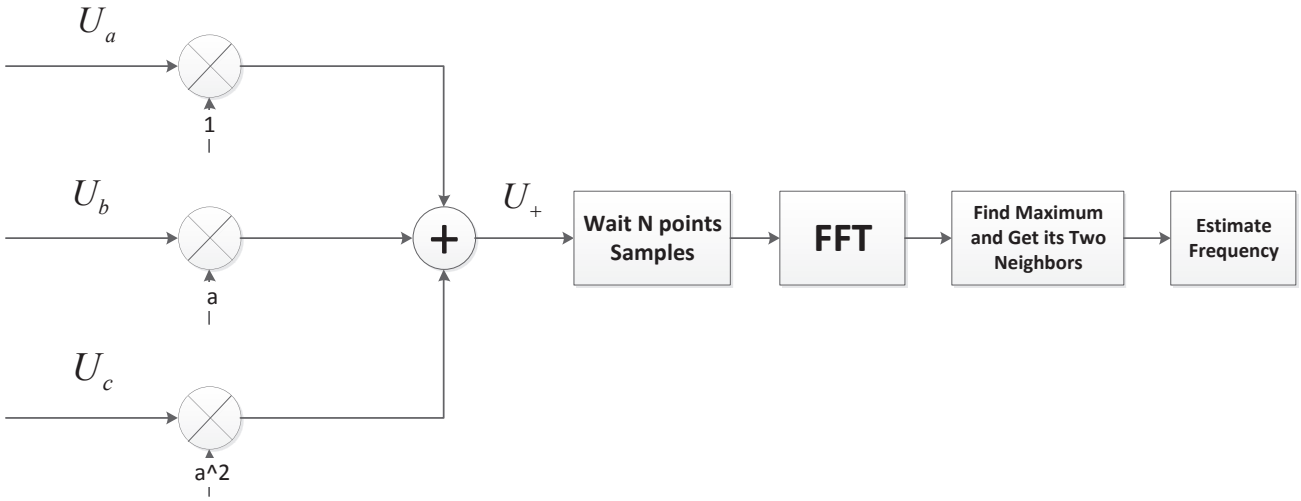

Fig. 2. The procedure of proposed algorithm starting in balanced three-phase power system

A. Bias Comparisons

The bias is defined as $b = |\mathbf{E}\{\hat{\delta}\} - \delta|$. In [7], it has already been shown that the algorithm proposed there has the best bias performance. Therefore, in this subsection, we will only compare the bias among our proposed algorithms and that in [7].

In the noiseless case, the analytical bias of our proposed algorithm has been calculated by Eq. (22). Fig. 3(a) shows the bias with observation length $N = 8$. It can be observed that the bias is a periodic function of the signal frequency, f. This phenomenon comes from Eq. (22), which states that the analytical bias is a function of δ, which is a periodic function of the frequency, f. Since different f may correspond to the same δ with different k_m, we see that the bias periodic in f. In addition, it can be observed that within a period, the bias b_δ is a monotonically increasing function of $|\delta|$, as stated in Eq. (4). Moreover, as Eq. (4) shows, the estimated frequency is a function of frequency resolution Δf. For the same window length, the frequency resolution of our proposed algorithm is one half of Candan's [7] because of the zero-padding in our method. Furthermore, as shown from Eq. (22), the bias is an inversely proportional function of the observation window length N. Therefore, a longer observation window will result in a better performance. This can be justified by comparing Figs. 3(a) and 3(b), where Fig. 3(b) shows the bias in the noise free case with observation window size $N = 32$.

B. RMSE Performances

In this part, the RMSE defined as $\sqrt{\mathbf{E}[(\delta - \hat{\delta})^2]}$, are compared among the proposed methods and existing ones. In [5] and [6], the Cramer-Rao lower bound for unbiased estimator of the frequency of a single-tone signal was derived. Though estimators that use interpolation of DFT coefficients are usually not unbiased, Cramer-Rao lower bound is still a good indicator of the performance of such estimators. Thus, in this section, we will plot the Cramer-Rao bound as a reference for the simulation comparisons.

As Figs. 4(a), 4(b), 5(a) and 5(b) show, our proposed algorithms have the best performance for any given SNR. At low SNR, Candan's and our proposed algorithm, and their corresponding iterative versions have the same

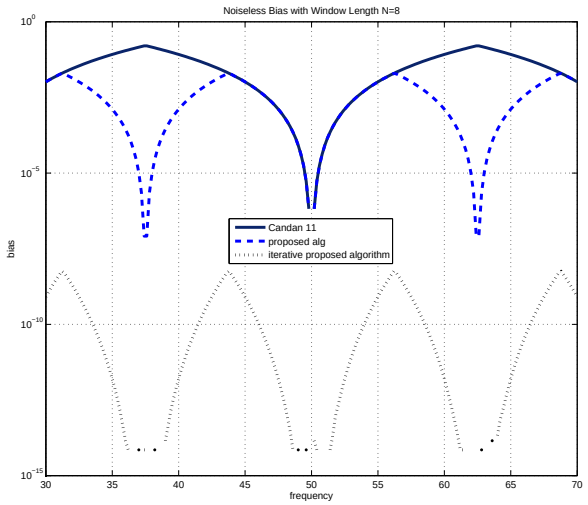

(a) Bias of Window Length N=8

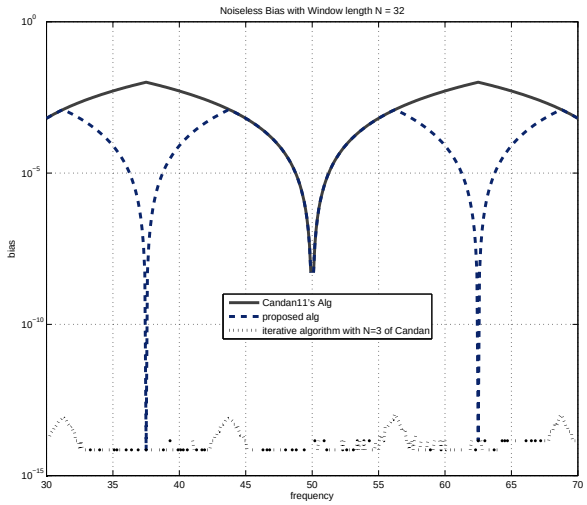

(b) Bias of Window Length N=32

Fig. 3. Noiseless Bias vs Frequency Comparison: The solid line is algorithm proposed in [7]; The dash line is based on Eq. (21); The dot line is based on Eq. (27)

performance, where the iterative algorithm takes three iterations. This is because at low SNR, the bias value is too small to dominate the RMSE. However, compared to other existing algorithms, our algorithms still have the best performance at low SNR. In fact, as shown in Fig.4 where $N = 8$, there is a gain of almost 2 dB with our algorithm, compared to Candan's [7]. The gain G is calculated as follows:

$$G = 20 \log_{10} \frac{\text{RMSE}_c}{\text{RMSE}_p}$$

Where the subscripts c and p corresponds to Candan's algorithm [7] and our proposed one, respectively. However, at high SNR, the performance of proposed iterative is obvious, since the bias dominates the RMSE. Because of the same reason, both our proposed algorithm and Candan's have error floor at high SNR. It can also be observed from Figs. 3 that the no-bias-compensated versions of Candan's [7] and our proposed algorithms has the same error floor performance. However the bias-compensated version of our algorithm have lowest RMSE among three estimators at high SNR.

C. Test with Standard

In standard C37.118.1-2011 [3], the evaluation of frequency estimators is based on absolute frequency measurement error (FE), defined as follows:

$$\text{FE} = |f_{true} - f_{measure}| \tag{28}$$

which is the similar as bias definition in noiseless case. The standard also defines the measurement reporting latency, which is maximum time interval between the data report time, as indicated by the data time stamp, and the time when the mesurements become available at the PMU output. In fact, the reporting latency involves many factors, such as the window over which data is gathered to make a measurement, the PMU processing time, the estimation method and so on. According to our proposed algorithm, the most time-consuming operation is finding the maximum on frequency domain. However, as our proposed method can work on short window length as in Fig.

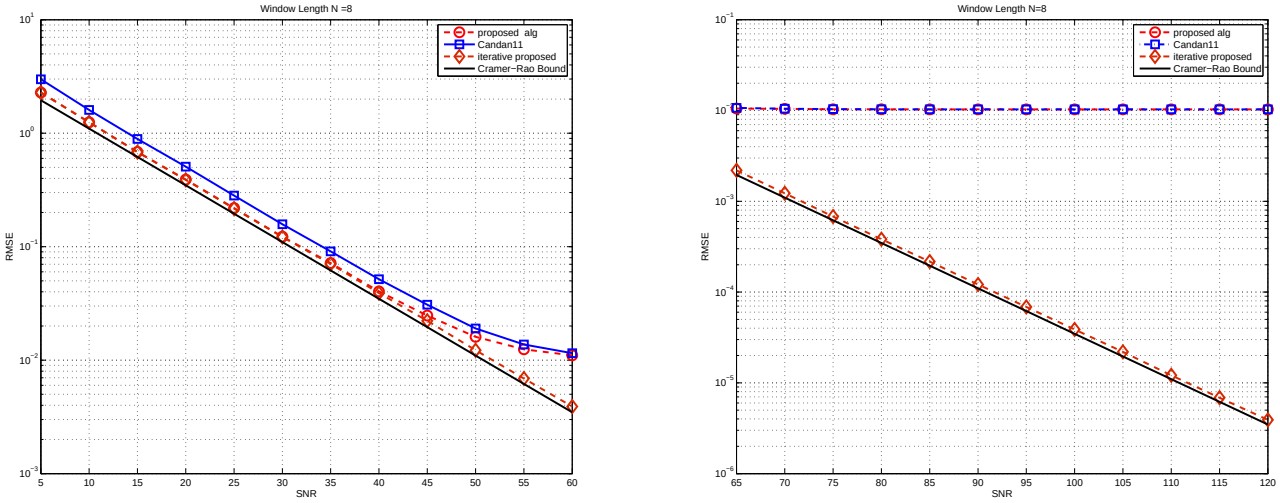

(a) RMSE in low SNR

(b) RMSE in high SNR

Fig. 4. RMSE vs.SNR Comparison in Power System: The solid line with square marker is algorithm proposed in [7]; The dash line with circle marker is Eq. (21); And the dash line with diamond marker is Eq. (27)

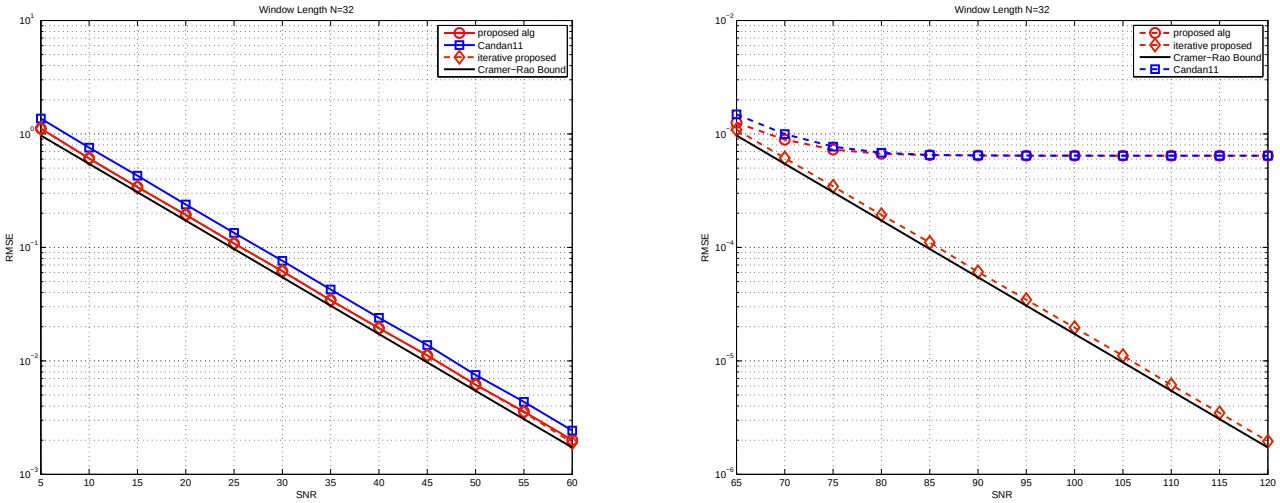

(a) RMSE in low SNR

(b) RMSE in high SNR

Fig. 5. RMSE vs.SNR when $N = 32$: The solid line with square marker is algorithm proposed in [7]; The dash line with circle marker is Eq. (21); And the dash line with diamond marker is Eq. (27)

3, this operation time could be considered neglected . Furthermore, compared to the data gathering time, the PMU processing time can be omitted, so the measurement reporting latency can be simplified as data-gathering time. As the standard defined, the largest frequency deviation (defined as $\Delta f = f_{true} - f_{nominal}$) is at most 5 Hz. In this case, the strictest requirement in the standard is 0.005 Hz in frequency error. Table I shows the performance of our proposed algorithm, with respect to different sampling frequencies and window lengths. As shown in Fig. 3, the larger the deviation from nominal frequency is, within the range of one half of the frequency resolution, the bigger the frequency error is. Within the largest deviation of true frequency, the case where the true frequency is 65Hz or 55Hz has the worst performance. Therefore, in Table. I, only the cases where frequency is at 65Hz are

TABLE I
NOISELESS STEADY STATE TEST

f_{true} (Hz)	δ_{true}	f_s (Hz)	N	$\hat{\delta}$	$\hat{f}$ (Hz)	Freq. Error	responding time (sec)
65	0.1667	480	8	0.1667	65.0018	0.0018	0.0167
65	0.3333	480	16	0.3335	65.0018	0.0018	0.0333
65	0.1667	960	16	0.1667	65.0004	0.0004	0.0167
65	0.3333	960	32	0.3334	65.0004	0.0004	0.0333
65	0.1667	1920	32	0.1667	65.0001	1.1156×10^{-4}	0.0333

shown. As Table I shows, our proposed algorithm can meet the requirements of 0.005Hz in Frequency error (FE) in the steady state.

VI. CONCLUSION

In this report, we first analyzed some factors involved into frequency estimation. After that, we proposed a new frequency estimation algorithm by estimating the gap between the location of the maximum of DFT and the true frequency from the DFT of the zero-padded signal. Then, bias of our proposed algorithm was investigated. With the above analysis of bias, the bias-compensated algorithm was proposed based on the estimated result of the first proposed algorithm. The simulations showed that our proposed algorithm has the best performance at any SNR. In addition, our algorithm can satisfy the steady-state requirements of standard C37.118.1, with short observation window, such as $N = 8$.

ACKNOWLEDGEMENT

the authors would like to acknowledge and extend heartfelt gratitude to Robert Griffin for his suggestions on English writing.

REFERENCES

[1] M. H. Bollen and I. Y. Gu, *Signal Processing of Power Quality Disturbances*. Wiley-IEEE Press, 2006.

[2] IEEE Std C37.118, *IEEE Standard for Synchrophasors for Power Systems*, 2005.

[3] "IEEE standard for synchrophasor measurements for power systems," *IEEE Std C37.118.1-2011 (Revision of IEEE Std C37.118-2005)*, pp. 1 –61, 28 2011.

[4] "IEEE standard for synchrophasor data transfer for power systems," *IEEE Std C37.118.2-2011 (Revision of IEEE Std C37.118-2005)*, pp. 1 –53, 28 2011.

[5] D. Rife and R. Boorstyn, "Single tone parameter estimation from discrete-time observations," *IEEE Trans. on Information Theory*, vol. 20, pp. 591 – 598, September 1974.

[6] M. Macleod, "Fast nearly ML estimation of the parameters of real or complex single tones or resolved multiple tones," *IEEE Trans. on Signal Processing*, vol. 46, pp. 141 –148, January 1998.

[7] C. Candan, "A method for fine resolution frequency estimation from three DFT samples," *IEEE Signal Processing Letters*, vol. 18, pp. 351 –354, June 2011.